Correction to Thermodynamic Characterization of a Thermostable Antibiotic Resistance Enzyme, the Aminoglycoside Nucleotidyltransferase (4′)

ARTICLE *in* BIOCHEMISTRY · OCTOBER 2012

Impact Factor: 3.02 · DOI: 10.1021/bi301126g · Source: PubMed

BIOCHEMISTRY
including biophysical chemistry & molecular biology

Article

pubs.acs.org/biochemistry

Thermodynamic Characterization of a Thermostable Antibiotic Resistance Enzyme, the Aminoglycoside Nucleotidyltransferase (4′)

Xiaomin Jing, Edward Wright, Amber N. Bible, Cynthia B. Peterson, Gladys Alexandre, Barry D. Bruce, and Engin H. Serpersu*

Department of Biochemistry and Cellular and Molecular Biology, The University of Tennessee, 1414 Cumberland Avenue, Knoxville, Tennessee 37996, United States

Supporting Information

ABSTRACT: The aminoglycoside nucleotidyltransferase (4′) (ANT) is an aminoglycoside-modifying enzyme that detoxifies antibiotics by nucleotidylating at the C4′-OH site. Previous crystallographic studies show that the enzyme is a homodimer and each subunit binds one kanamycin and one Mg-AMPCPP, where the transfer of the nucleotidyl group occurs between the substrates bound to different subunits. In this work, sedimentation velocity analysis of ANT by analytical ultracentrifugation showed the enzyme exists as a mixture of a monomer and a dimer in solution and that dimer formation is driven by hydrophobic interactions between the subunits. The binding of aminoglycosides shifts the equilibrium toward dimer formation, while the binding of the cosubstrate, Mg-ATP, has no effect on the monomer−dimer equilibrium. Surprisingly, binding of several divalent cations, including Mg^{2+}, Mn^{2+}, and Ca^{2+}, to the enzyme also shifted the equilibrium in favor of dimer formation. Binding studies, performed by electron paramagnetic resonance spectroscopy, showed that divalent cations bind to the aminoglycoside binding site in the absence of substrates with a stoichiometry of 2:1. Energetic aspects of binding of all aminoglycosides to ANT were determined by isothermal titration calorimetry to be enthalpically favored and entropically disfavored with an overall favorable Gibbs energy. Aminoglycosides in the neomycin class each bind to the enzyme with significantly different enthalpic and entropic contributions, while those of the kanamycin class bind with similar thermodynamic parameters.

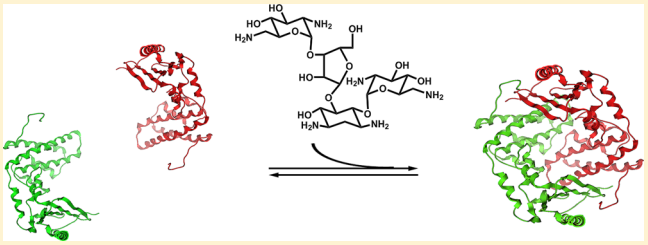

Aminoglycoside antibiotics (AGs) are pseudosaccharides, and a majority of them contain a central 2-deoxystreptamine group with attached sugars (Figure 1). Several classes of aminoglycosides, including gentamycins, kanamycins, and neomycins, function as antibiotics by binding to the 16S RNA of the 30S ribosomal subunit, which causes mistranslations and premature stops leading to cell death.[1,2] A large number of enzymes expressed in bacteria are capable of modifying aminoglycosides and rendering them ineffective as antibiotics.

Aminoglycoside-modifying enzymes (AGMEs) are classified as acetyltransferases, nucleotidyltransferases, or phosphotransferases.[2−4] Nucleotidyltransferases are the less abundant among the three types of aminoglycoside-modifying enzymes and generally have more limited substrate profiles. They catalyze the covalent attachment of nucleotide monophosphate to hydroxyl groups of aminoglycosides via a metal-ATP cofactor. To date, there are only a few studies describing enzymatic and thermodynamic properties of these enzymes.[5−10] In this work, we have used a previously described kanamycin resistance gene[11] from the thermophilic bacterium *Bacillus stearothermophilus* that encodes a thermostable kanamycin nucleotidyltransferase. Prior to use, this gene was modified to be codon-optimized for expression in *Thermosynechococcus elongatus*.[12] This thermostable variant of the aminoglycoside nucleotidyltransferase (4′) (ANT) was found to confer resistance to a large number of aminoglycosides.[6] A crystal structure is available for an ANT variant, D80Y T130K, which was determined at 3.0 Å resolution in the absence of substrates.[13] Additionally, the structure of the D80Y variant was determined at 2.5 Å resolution with kanamycin and Mg-AMPCPP.[14] Both the apo and substrate-bound structures are homodimers that are highly similar with a 0.75 Å root-mean-square deviation of superimposed α-carbon positions. Each monomer is shown to bind both the antibiotic and the metal-bound nucleotide (Figure 2). The binding sites for both substrates are solvent-exposed and contain charged residues contributed by both subunits, establishing an active site between the two protein monomers. The orientation of substrates facilitates the transfer of the nucleotidyl group between the substrates bound to different monomers. In this paper, we describe unique features of subunit−subunit interactions that are differentially affected by substrates, as well as the thermodynamic properties of enzyme−aminoglycoside complexes. Data presented here represent the first characterization of the thermodynamic properties of a thermostable variant of AGMEs.

Received: August 20, 2012
Revised: October 10, 2012
Published: October 15, 2012

dx.doi.org/10.1021/bi301126g | *Biochemistry* 2012, 51, 9147−9155

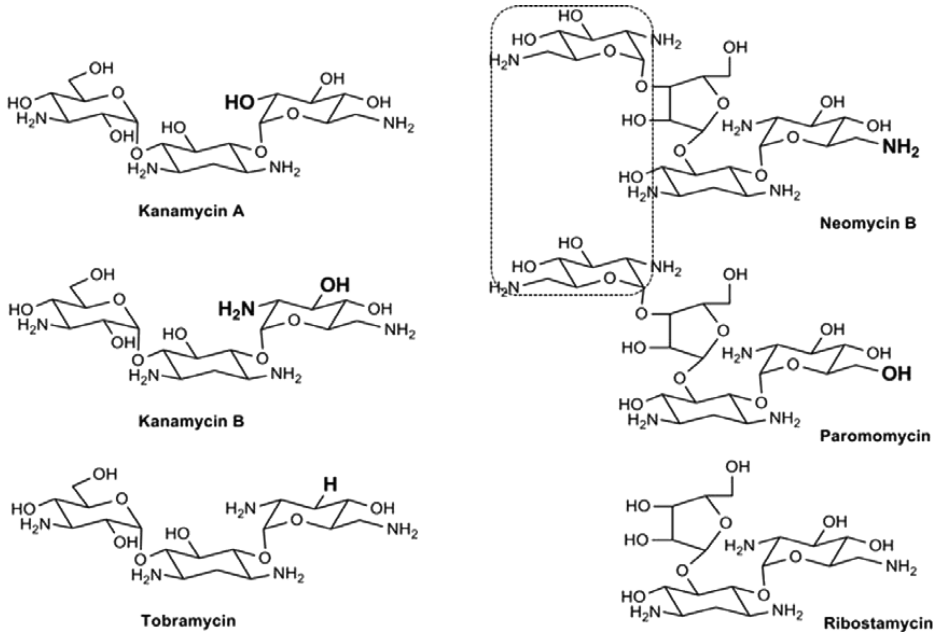

Figure 1. Chemical structures of aminoglycoside antibiotics. Ring D of the neomycin class is shown within the dotted rectangle. Kanamycin A, kanamycin B, and tobramycin are aminoglycosides with a 4,6-disubstituted ring, and neomycin, paromomycin, and ribostamycin are aminoglycosides with 4,5-disubstituted central 2-deoxystreptamine rings.

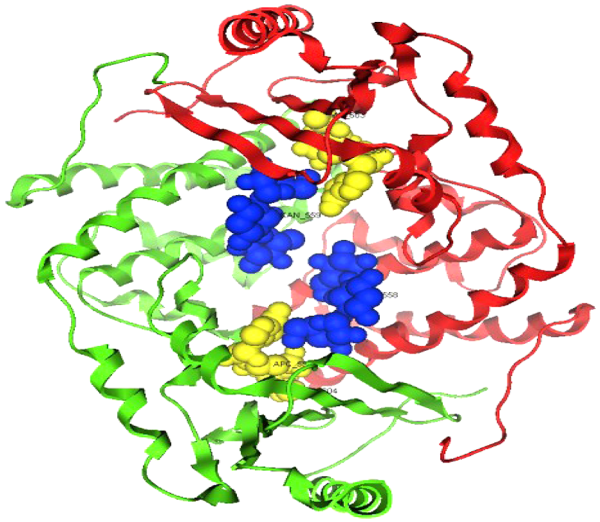

Figure 2. Backbone of the ANT D80Y T130K variant in ribbon representation. Two monomer subunits are colored red and green. Bound kanamycin A molecules are colored blue, and Mg-AMPCPP molecules are colored yellow (Protein Data Bank entry 1KNY).[14]

MATERIALS AND METHODS

Reagents. All materials were of the highest purity commercially available and were purchased from Sigma-Aldrich Co. (St. Louis, MO) unless otherwise noted. Ni^{2+} Sepharose High Performance resin was purchased from GE Healthcare (formerly Amersham, Piscataway, NJ). The Marco-Prep High Q Support strong anion exchange column was purchased from Bio-Rad Laboratories (Hercules, CA). Thrombin, prepared from thrombostat by cation exchange chromatography as described previously,[15] was graciously provided by E. Fernandez (The University of Tennessee).

Protein Expression and Purification. A thermostable variant of ANT, D80Y T130K, was obtained from thermophilic cyanobacteium *T. elongatus*. The target gene was inserted into a pET14b vector with an N-terminal six-His tag and transformed into an *Escherichia coli* BL21(DE3) pLysS cell line. Bacteria containing the plasmid were selected on LB plates with 50 μg/mL ampicillin and 34 μg/mL chloramphenicol. Cells were grown at 37 °C, induced with 1 mM IPTG, and harvested after being induced for 4 h. Cells were resuspended in 50 mM Tris-HCl (pH 7.5), 100 mM NaCl, and 1 mM EDTA and lysed by three freeze−thaw cycles. The lysate was treated with DNase for 1 h and centrifuged at 14000 rpm for 30 min. ANT, carrying a His tag consisting of six histidines, was isolated by Ni^{2+} affinity chromatography. The six-His tag was removed by thrombin cleavage for 1 h at room temperature. Following cleavage, the protease was removed by chromatography over a strong anion exchange resin. Fractions containing ANT were pooled and dialyzed against 50 mM PIPES buffer (pH 7.5), concentrated by ultrafiltration, and stored at 4 °C. Under these conditions, the enzyme remained active for several weeks. Protein concentrations were determined by absorbance at 280 nm using an extinction coefficient of 50880 M^{-1} cm^{-1}. Protein concentrations are reported as monomer concentrations unless otherwise indicated.

Analytical Ultracentrifugation (AUC). Sedimentation velocity experiments were performed in a Beckman XL-I analytical ultracentrifuge using an An-50Ti rotor. Sample volumes of 400 μL were loaded into double-sector cells and allowed to equilibrate for 1 h at 25 °C prior to the run. Absorbance scans at 280 nm were collected at a rotor speed of 50000 rpm and 25 °C. Sedimentation data were fit to a continuous $[c(s)]$ distribution model using SEDFIT (version 12.44).[16] The protein partial specific volume, buffer density, and buffer viscosity were calculated using SEDNTERP.[17]

Prior to all experiments, the enzyme was dialyzed extensively against the buffer of interest. For analysis of salt-dependent and concentration-dependent dimerization of ANT, the buffer contained 50 mM PIPES (pH 7.5) and variable concentrations of NaCl. For analysis of aminoglycoside-dependent, nucleotide-

dx.doi.org/10.1021/bi301126g | *Biochemistry* 2012, 51, 9147−9155

dependent, and divalent cation-dependent dimerization, the buffer contained 50 mM PIPES (pH 7.5) and 100 mM NaCl. For pH dependence, a triple-buffer system (10 mM MES, 10 mM HEPES, and 10 mM BICINE with 50 mM NaCl) was used to minimize any non-pH-related effects arising from the use of different buffer components. For temperature dependence, the buffer consisted of 50 mM MOPS (pH 7.5) and 50 mM NaCl. To evaluate the effect of metals on the monomer−dimer equilibrium of this enzyme, 2.0 mM Mg^{2+}, Mn^{2+}, or Ca^{2+} was added to 10 μM ANT.

For quantitative analysis of the monomer−dimer equilibrium of ANT, a protein concentration range of 1−40 μM was used. Different detection strategies were required to maximize sensitivity and ensure that measurements were within the linear region over this concentration range. At lower concentrations (1.0−3.5 μM), absorbance at 230 nm was used to monitor sedimentation. Absorbance data at 280 nm were acquired for ANT at 5−20 μM, and at 40 μM enzyme, the interference optical system was used for detection. For data analysis, the weight-average sedimentation coefficients $[s_w(S)]$ were determined at each concentration by integrating the peaks from the $c(s)$ distributions using SEDFIT.[16] Isotherm analysis of $s_w(S)$ as a function of protein concentration with the monomer−dimer self-association model in SEDPHAT was employed to determine the dissociation constant.[18] The values from isotherm analysis were used as the initial guesses in global analysis to determine the kinetics of the interaction.[18,19] For the determination of k_{off}, multiple data sets were analyzed in SEDPHAT using a form of the Lamm equation that explicitly incorporates the reaction kinetics occurring during sedimentation.[20] All reported errors from data analyses with SEDPHAT were generated using the F statistic calculator.

Electron Paramagnetic Resonance. Continuous-wave X-band (9.78 GHz) EPR spectra of free Mn^{2+} were recorded by using a Bruker (Billerica, MA) EMX spectrometer. All EPR experiments were performed at room temperature using a thin wall quartz capillary with a volume of 80 μL. Spectra were collected with a 20 mW power, a 100 kHz modulation frequency, a 4.0 G modulation amplitude, and four scans. All the samples were prepared in 50 mM Pipes and 100 mM NaCl (pH 7.5). The enzyme concentration was 60 μM for all EPR experiments, and the manganese concentration ranged from 10 to 300 μM. To observe the effect of aminoglycoside on metal binding, the concentration of neomycin was adjusted to 100 μM to achieve >99% enzyme saturation.

Isothermal Titration Calorimetry. ITC experiments were performed at 25 °C using a VP_ITC mircocalorimeter from Microcal, Inc. (Northampton, MA). The concentrations of aminoglycoside antibiotics were determined by the enzymatic assay with aminoglycoside acetyltransferase(3)-IIIb as described previously.[21] Both enzyme and ligand solutions were degassed under vacuum for 10 min at 20 °C. Titrations consisted of 27 injections of 10 μL and were separated by 240 s, and a cell stirring speed of 300 rpm was used. For each titration, the ANT concentration was 20 μM, resulting in c values (enzyme concentration × K_{assoc}) ranging from 1.3 to 100, with the exception of that of neomycin, which is 100. These values fall within the acceptable range (1−1000) for determining binding constants by ITC.[22] The observed heat change (ΔH) evolving from binary complex formation and the binding affinity were directly determined from titration. Free energy (ΔG) and entropy (ΔS) changes associated with binding were determined from eqs 1 and 2. All data were fit to a single-site binding model using Origin 5.0 from Microcal, Inc.

$$\Delta G = -RT \ln K_a \quad (1)$$

$$\Delta G = \Delta H - T\Delta S \quad (2)$$

Determination of the intrinsic enthalpy of binding was done as described previously.[23] Briefly, the following equation was used to evaluate and subtract the contribution, if any, by pK_a shifts of titratable sites:

$$\Delta H_{obs} = \Delta H_{int} + \Delta H_{ion}\Delta n \quad (3)$$

where ΔH_{obs} is the observed enthalpy change, ΔH_{ion} is the heat of ionization of the buffer, and Δn is the net transfer of protons by the buffer upon formation of the complex. ΔH_{int} and Δn are determined from the intercept and slope, respectively. Under these experimental conditions, a net proton uptake by the enzyme−ligand complex yields a positive Δn.

RESULTS AND DISCUSSION

ANT Is in Equilibrium between Monomeric and Dimeric Forms. Initial sedimentation velocity data with 5 μM ANT in the absence of substrates showed a broad peak with a sedimentation coefficient (S) of 3.7 and a frictional coefficient (f/f_0) of 1.17. These values result in a molecular mass of 43.2 kDa, which is intermediate between those of the monomeric (28.9 kDa) and dimeric species of this protein. Subsequent experiments showed a concentration-dependent increase in S (Figure 3). These observations suggested that the apoenzyme is in equilibrium between monomer and dimer species with fast association−dissociation kinetics relative to the time scale of the sedimentation experiment. Therefore, the observed peak positions reflect the weight-average S of monomeric and dimeric species.

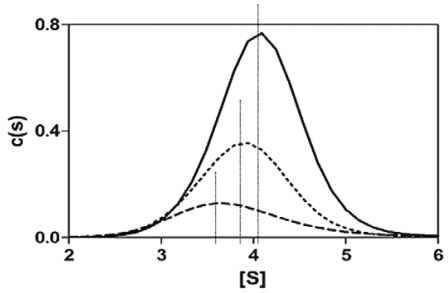

Figure 3. Size distribution of apo-ANT at different concentrations. Dashed, dotted, and solid lines represent data for 5, 10, and 20 μM ANT, respectively. All the runs were performed in 50 mM PIPES (pH 7.5) and 100 mM NaCl.

The weight-average sedimentation coefficients were plotted as a function of protein concentration to determine the distribution of species and the monomer−dimer equilibrium constant. Figure 4 shows isotherm analysis using the data acquired with an enzyme concentration range of 1−40 μM. The data were fit to the monomer−dimer self-association model in SEDPHAT.[18] The curve represents the best fit to the data points that yields a dissociation constant of 1.7 ± 0.4 μM for the dimer and sedimentation coefficients of 2.7 and 4.4 S for the monomer and dimer, respectively. Global analysis of the sedimentation velocity data acquired at 280 nm showed the dissociation rate constant (k_{off}) to be on the order of 10^{-2} s^{-1} for the ANT dimer in the absence of substrates (Figure 4).

dx.doi.org/10.1021/bi301126g | Biochemistry 2012, 51, 9147−9155

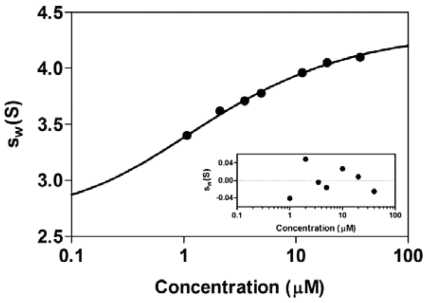

Figure 4. Isotherm of the weight-average sedimentation coefficient as a function of ANT concentration. The fitted curve is shown with the original data points. The monomer−monomer self-association model was utilized to characterize the dissociation constants and sedimentation coefficients of two species. The inset shows the residuals.

Binding of Aminoglycosides Promotes the Dimerization of ANT. The crystal structure of ANT shows that the C4′-OH group of kanamycin is ∼5 Å from the α-phosphorus of the nucleotide bound to the opposite subunit (Figure 2). This is an optimal orientation for a direct nucleophilic attack to facilitate nucleotide transfer. However, the distance between the substrates bound to the same monomer is ∼24 Å, indicating that the enzyme must be in its dimeric form to catalyze the reaction.[14] Because solution studies showed that the enzyme exists in equilibrium between the monomeric and dimeric forms, we evaluated the effect of various factors on this equilibrium. First, two different substrates, kanamycin and neomycin B (henceforth neomycin), representing each of the two major structurally different groups of aminoglycoside antibiotics (Figure 1), were tested. As shown in Figure 5, increasing concentrations of either aminoglycoside cause a clear shift to higher S values. These results demonstrate that aminoglycosides shift the equilibrium heavily in favor of dimer formation. Additionally, both antibiotics slow the dissociation rate of the dimer by >100-fold ($k_{off} \geq 10^{-4}$ s^{-1}). Unlike the apoenzyme, two separate signals for the monomer and dimer are clearly visible in binary enzyme−aminoglycoside complexes, confirming the slow dissociation rates of the dimer in the presence of both antibiotics. Neomycin is able to achieve this effect at lower concentrations, reflecting the tighter binding of neomycin versus that of kanamycin A. An additional 2.5-fold increase in the neomycin concentration above the saturation level did not lead to the formation of any higher-order complexes. In contrast, the binding of the cosubstrate Mg-ATP to the enzyme does not lead to dimerization of the enzyme . These data are consistent with the kinetic studies that showed that substrate binding is ordered when the aminoglycoside binds before the nucleotide.[6] Thus, the binding of an aminoglycoside to the enzyme induces the formation of the "active" form of the enzyme.

Binding of Divalent Cations to ANT Induces Enzyme Dimerization. In the absence of substrates, the sedimentation velocity results show an increase in the sedimentation coefficient consistent with almost complete dimerization for all three of the divalent cations tested (Mg^{2+}, Mn^{2+}, and Ca^{2+}). These observations are consistent with the crystal structure of the apoprotein that showed a dimeric protein with a divalent cation bound to each monomer,[13] which was proposed to be Zn^{2+}. However, other transition metals were also consistent with the observed electron density. Our attempts to test the effect of Zn^{2+} were unsuccessful because the presence of millimolar concentrations of zinc caused precipitation of the enzyme under our experimental conditions.

In an attempt to clarify the effects observed with Mg^{2+} versus Mg-ATP, experiments were conducted with ATP in sufficient excess of Mg^{2+} to ensure that all Mg^{2+} was in complex with ATP. In these experiments, no effect on the monomer−dimer equilibrium was observed, indicating that free Mg^{2+} binds to a site different from that of Mg-ATP. To gain insight into the binding of the divalent cations to the apoenzyme, we used electron paramagnetic resonance (EPR) spectroscopy. Paramagnetic Mn^{2+} was used as the EPR probe. In aqueous solution, free manganese gives a sharp concentration-dependent EPR signal. When the metal binds to the protein, the signal broadens to undetectable levels. Titration of the enzyme with Mn^{2+} showed that Mn^{2+} binds to ANT with a dissociation constant of 100 ± 20 μM and an Mn^{2+}:enzyme stoichiometry of 2:1. In the crystal structure of apo-ANT, two cations were observed in symmetrical locations between the carboxylate groups of two glutamate residues (E76 and E145) from opposite monomers.[13] In the substrate-bound structure, these two residues were shown to make important contacts with the aminoglycoside.[14] To test whether aminoglycoside inhibits metal binding, the Mn^{2+} binding experiment was repeated in the presence of neomycin. The presence of the aminoglycoside prevented binding of Mn^{2+} to the enzyme (Figures S1 and S2 of the Supporting Information), suggesting that the divalent cations exert their effect on the monomer−dimer equilibrium

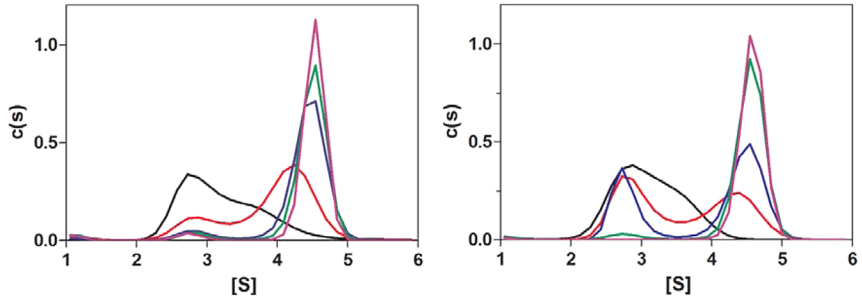

Figure 5. Effect of aminoglycosides on the monomer−dimer equilibrium of ANT. AUC data for kanamycin (left) and neomycin (right) complexes as a function of the increased level of saturation of ANT with antibiotics (black, no aminoglycoside; saturation progressively increases with colors orange, blue, green, and red, where red represents full saturation). For kanamycin, the lines represent 0, 45, 85, 95, and >97% saturation of ANT, respectively. For neomycin, the lines correspond to 0, 20, 50, 95, and >98% saturation, respectively. Experiments were performed at 25 °C in 50 mM PIPES (pH 7.5) containing 100 mM NaCl.

dx.doi.org/10.1021/bi301126g | *Biochemistry* 2012, 51, 9147−9155

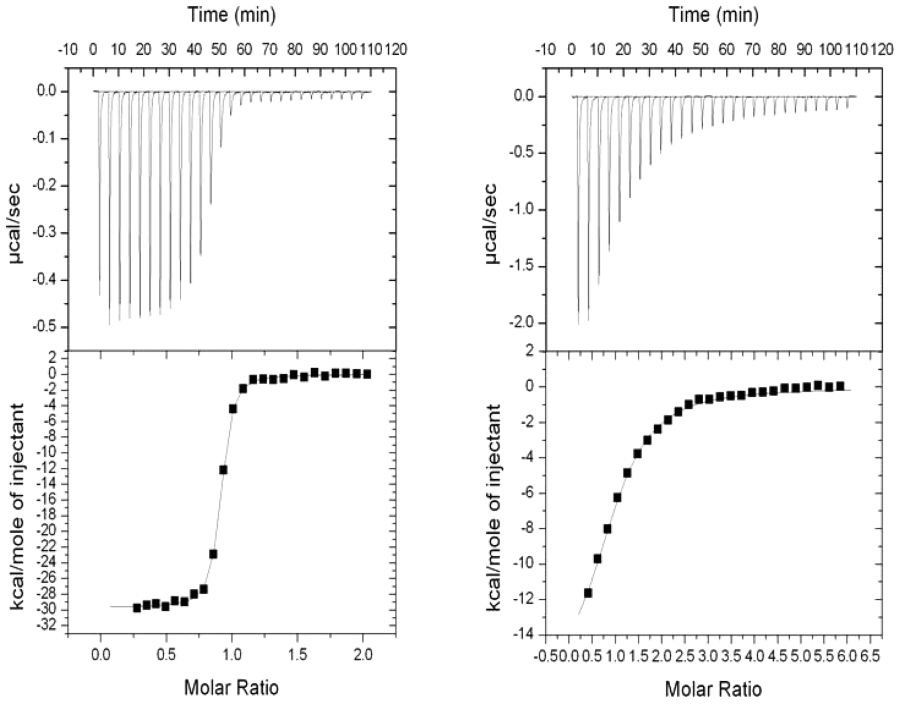

Figure 6. Thermograms (top) and isotherms (bottom) obtained from the titration of aminoglycosides (left, neomycin; right, kanamycin A) into a solution containing 20 μM ANT in 50 mM PIPES (pH 7.5) and 100 mM NaCl at 25 °C. In both cases, the best fit was obtained from a single-site binding model.

Table 1. ITC-Derived Thermodynamics of Aminoglycoside Binding[a]

	K_d (μM)	ΔH_{int} (kcal/mol)	$T\Delta S$ (kcal/mol)	ΔG (kcal/mol)	Δn
kanamycin A	6.6 ± 1.1	−20.7 ± 0.4	−13.6	−7.1 ± 0.1	1.4 ± 0.1
kanamycin B	4.6 ± 1.6	−22.7 ± 2.8	−15.4	−7.3 ± 0.3	1.3 ± 0.5
tobramycin	1.1 ± 0.3	−19.3 ± 1.4	−11.2	−8.1 ± 1.0	1.4 ± 0.2
neomycin	0.02 ± 0.01	−32.0 ± 0.6	−22.3	−10.4 ± 0.3	2.0 ± 0.1
paromomycin	0.2 ± 0.04	−38.0 ± 1.8	−28.9	−9.1 ± 0.1	2.4 ± 0.2
ribostamycin	15.4 ± 4.2	−12.6 ± 1.2	−6.0	−6.6 ± 0.2	0.7 ± 0.2

[a]Errors in the intrinsic enthalpy (ΔH_{int}) and in net protonation (Δn) were derived from the deviation from linearity of observed enthalpies as a function of the heat of ionization of the buffer used. Data and errors in the Gibbs energy (ΔG), entropy ($T\Delta S$), and dissociation constant (K_d) were calculated from the average of three to six trials, with errors being the standard error of the mean. In all the cases, the best fit was obtained by using the single-site binding model.

through the antibiotic binding site, which is rich in negatively charged titratable groups.

Effects of Salt, pH, and Temperature on Equilibrium. Other factors were tested in sedimentation velocity experiments to gain insight into the nature of the dimerization process of ANT. Increasing the salt concentration favored the formation of the dimer. Because the dimerization interface consists of primarily complementary electrostatic interactions and hydrophobic interactions, an increased level of dimerization with an increasing salt concentration suggests that hydrophobic interactions are the major cause of dimer formation. These data do not exclude the possibility that high salt could be shielding repulsive ionic interactions to promote dimerization (Figure S2 of the Supporting Information). However, neither pH changes between pH 6.5 and 8.5 nor the temperature range between 15 and 35 °C showed a significant effect on the monomer−dimer equilibrium.

Thermodynamic Properties of Aminoglycoside−Enzyme Complexes. Thermodynamic parameters of the binary enzyme−aminoglycoside complexes were determined by isothermal titration calorimetry (ITC) using six different aminoglycosides representing two major groups of aminoglycoside antibiotics, kanamycins and neomycins (Figure 1). Experimental conditions were selected to ensure that the predominant form of the apoenzyme was a dimer. Therefore, the heat of dimerization, if any, should not contribute significantly to the observed enthalpy. Furthermore, separate experiments showed that no detectable heat was observed as a concentrated enzyme solution was diluted into the ITC cuvette, suggesting that the heat of dimerization was very small. A typical ITC data set for the binding of two aminoglycosides with highly different binding affinities for ANT is shown in Figure 6.

Binding of all aminoglycosides to ANT was enthalpically favored and entropically disfavored (Table 1) following the general trend observed with several different aminoglycoside-modifying enzymes.[21,23−28] Enthalpy−entropy compensation plots shown in Figure 7 yield a slope of 1.13 ± 0.1 indicating a slightly more significant role for enthalpy in the formation of the binary enzyme−aminoglycoside complexes. A $\Delta\Delta H/(-T\Delta\Delta S)$ slope of 1.0 would indicate than any increase in favorable enthalpy would be offset by a corresponding

dx.doi.org/10.1021/bi301126g | *Biochemistry* 2012, 51, 9147−9155

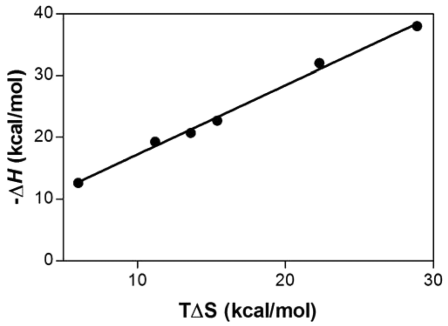

Figure 7. Enthalpy−entropy compensation plot. Data representing the intrinsic binding enthalpies from Table 1 were used to construct the plot.

unfavorable entropy. A slope of >1.0 shows that increased affinity correlates with enthalpy. In the context of aminoglycosides binding to ANT, a more favorable enthalpy from the number and strength of the hydrogen bonds to the enzyme and other factors is not countered by an equal decrease in the favorable ΔS, resulting from a loss of conformational and desolvation entropy. Prior to this work, such data with all other aminoglycoside-modifying enzymes yielded slopes in the range of 1.00−1.09.[21,25,26] Data acquired in this work show that ANT exhibits the most enthalpy-driven ligand binding among the AGMEs tested to date.

The binding enthalpy of kanamycins varied less than 3.5 kcal/mol with similar variations in entropy. This yielded similar Gibbs energies of binding for all three kanamycins, which are also reflected in the narrow range of dissociation constants for these aminoglycosides (Table 1). In contrast, the neomycin group aminoglycosides showed significant differences in most of the thermodynamic parameters.

One member of the neomycin group, ribostamycin, binds to ANT ∼800- and ∼80-fold weaker than neomycin and paromomycin, respectively. The binding enthalpy for ribostamycin was also significantly lower than those for the kanamycins. The binding affinity of ribostamycin was also the lowest among all antibiotics tested. These observations are likely due to the structure of ribostamycin, which is identical to that of neomycin but without the fourth ring (Figure 1). This ring could make a number of contacts with the enzyme, leading to the significantly more favorable enthalpy of binding observed with neomycin and paromomycin relative to that with ribostamycin. Because the crystal structure of the enzyme is available only with bound kanamycin, it is not easy to predict what interactions will occur between the enzyme and the neomycins to determine specifically the effect of the fourth ring. However, one may speculate that larger antibiotics such as neomycin and paromomycin would fit into the large active site cavity between the two subunits of the enzyme better than smaller aminoglycosides such as kanamycins and thus would make more favorable contacts with the enzyme. An analogous situation was observed with another aminoglycoside-modifying enzyme, the aminoglycoside *N*-acetyltransferase(3)-IIIb, in which the larger aminoglycosides with four rings (neomycin and paromomycin) bind to the enzyme with significantly more favorable enthalpies than three-ring aminoglycosides. The size of the active site cavity also affected the stoichiometry of binding of aminoglycosides to this enzyme such that three-ring aminoglycosides bind to the enzyme with stoichiometries of >1 while the complexes of larger aminoglycosides with the enzyme displayed a 1:1 stoichiometry, suggesting that bulkier aminoglycosides provide better fits to the large active site cavity of this protein as well.[21]

Binding of aminoglycosides to AGMEs is typically accompanied by changes in the net protonation caused by shifts in pK_a values of functional groups in both the enzyme and the ligand.[21,23,26] Therefore, we determined binding enthalpies in three different buffers with different heats of ionization to determine the intrinsic binding enthalpies (ΔH_{int}) and the change in net protonation (Δn) upon binding of aminoglycoside to ANT (Figure 8). Data showed that the net protonation remained the same with all three kanamycin group aminoglycosides, while significant differences were observed between the members of the neomycin group (Table 1). The net protonation was highest with paromomycin (2.4 ± 0.2) and neomycin (2.0 ± 0.1). The lowest value among all aminoglycosides also belongs to the neomycin group where ribostamycin has a Δn value of 0.7 ± 0.2. This suggests that the two amine functions in the fourth ring of neomycin and paromomycin may have upshifted pK_a values in the enzyme−aminoglycoside complexes and their contribution must be significant. Therefore, the lack of the fourth ring in ribostamycin excludes their contribution to the observed Δn. This is also consistent with the differences in binding enthalpies and suggests that multiple, strong interactions between the fourth ring in aminoglycosides and the enzyme exist. Other effects such as the contributions from the functional groups of the enzyme to the observed Δn, however, cannot be excluded. In fact, attribution of the changes in Δn to only the functional groups of the ligand is incorrect and has already been demonstrated with a different aminoglycoside-modifying

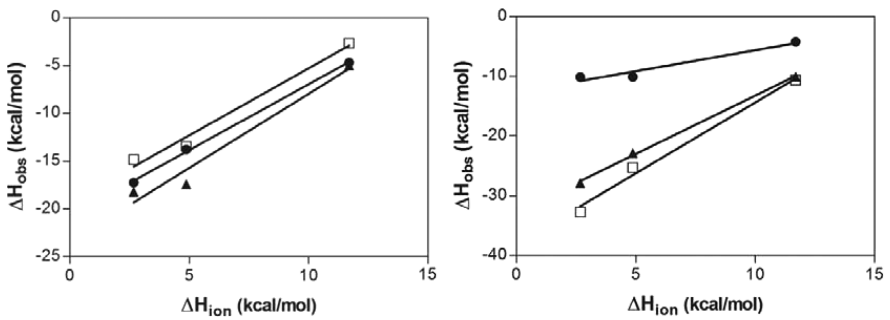

Figure 8. Effect of titratable groups on the observed enthalpy of binding. Observed enthalpies of kanamycins (left) and neomycins (right) as a function of the heat of ionization of the buffer used, 11.70 kcal/mol for Tris, 4.87 kcal/mol for HEPES, and 2.67 kcal/mol for PIPES. Left: tobramycin (□), kanamycin A (●), and kanamycin B (▲). Right: paromomycin (□), ribostamycin (●), and neomycin (▲).

dx.doi.org/10.1021/bi301126g | *Biochemistry* 2012, 51, 9147−9155

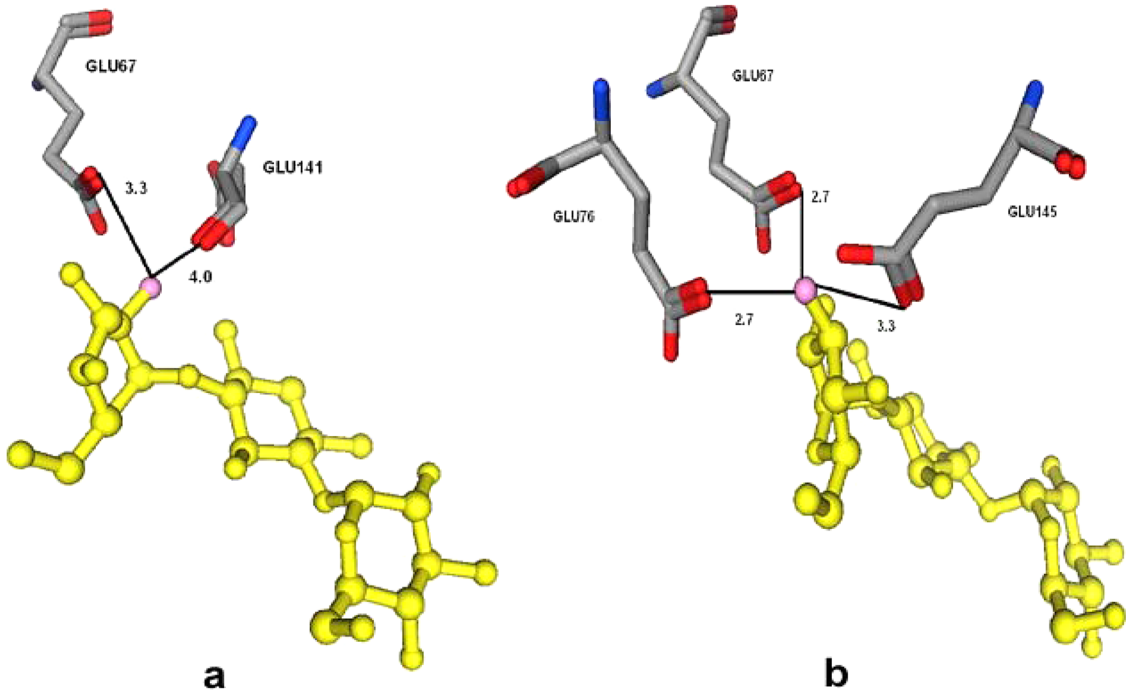

Figure 9. (a) Residue contacts of the kanamycin 2′-OH within 4.0 Å. E67 and E141 are shown as sticks. The yellow molecule in ball-and-stick representation is kanamycin A. O2′ is colored pink. (b) Residue contacts of the kanamycin A 3′-OH within 4.0 Å. E67, E76, and E145 are shown as sticks. The yellow molecule in ball-and-stick representation is kanamycin A. O3′ is colored pink.

enzyme.[23] Therefore, in the absence of data for the functional groups of the enzyme, any further attributions on the sites that may contribute to Δn will be misleading.

Aminoglycoside Recognition by ANT. Single-site differences between structurally similar aminoglycosides can lead to dramatic changes in the thermodynamic parameters of enzyme−aminoglycoside complexes.[29] If one compares the small differences in thermodynamic parameters of ANT−aminoglycoside complexes, it becomes clear that the change of the hydroxyl function (kanamycin A) to an amine (kanamycin B) at the C2′ site yields a 2 kcal/mol more favorable enthalpy, suggesting that the amine group makes an additional contribution to the enthalpy that may be due to ionic interactions with the enzyme. Two ionizable groups, E67 and E141, are the most likely candidates for the interaction of this site with the enzyme as they are 2.2 and 3.1 Å distant, respectively (Figure 9a). Although that represents a significant difference between the binding enthalpies of kanamycin A and kanamycin B, the observed 2 kcal/mol difference in ΔH_{int} between these two aminoglycosides is smaller compared to data acquired with other aminoglycoside-modifying enzymes,[21,25,26] suggesting that ANT is the least capable enzyme in differentiating these two aminoglycosides.

Comparison of ΔH_{int} of kanamycin B to tobramycin suggests that the replacement of the hydroxyl group at the C3′ site (kanamycin B) with hydrogen (tobramycin) lowers the binding enthalpy by 3.4 kcal/mol. Because the enthalpy of a hydrogen bond can be between 1 and 5 kcal/mol,[30,31] these data thus strongly suggest that the OH group at this site is involved in H-bond interactions. Three residues with a <4 Å distance from the C3′-OH group of kanamycin A are E67, E76, and E145 (Figure 9b) and are good candidates for this interaction. Thus, the observed 3.4 kcal/mol lowering of the binding enthalpy with tobramycin is consistent with the loss of one or two hydrogen bonds.

Comparison of neomycin and paromomycin reveals the contribution of the group at the C6′ position to the formation of the binary enzyme−aminoglycoside complex. It appears that this site makes the most significant impact on the binding of aminoglycosides to the enzyme among the three similar pairs and suggests that interactions of this site with the enzyme are more susceptible to changes. Substitution of C6′-OH with C6′-NH_2 in neomycin yields a 10-fold increase in binding affinity. The Gibbs energy for the binding of neomycin is more favorable despite the fact that binding of paromomycin to ANT is enthalpically favored by 5.3 kcal/mol over neomycin, which is slightly overcompensated by a more disfavorable entropy (Table 1).

The kanamycin-bound structure of ANT shows that there are no functional groups in the enzyme within a 4.0 Å distance of the C6′ site. The closest residue is E46, which is 4.9 Å distant. Therefore, the insertion of a charged group at this site must lead to an altered binding mode for the aminoglycoside or an altered conformation of the active site, which has a significant effect on the thermodynamic parameters of antibiotic association. The result is the significantly different thermodynamic properties observed with these two structurally similar aminoglycosides. Such significant differences between the thermodynamic properties of complexes formed with structurally similar aminoglycosides are not surprising. In fact, far more dramatic differences between the complexes of neomycin and paromomycin have been observed with another aminoglycoside-modifying enzyme, the aminoglycoside *N*-acetyltransferase(3)-IIIb, where the change in heat capacity showed opposite signs with these aminoglycosides.[29]

■ CONCLUSIONS

Although the binding pockets for both the aminoglycoside and nucleotide are composed of amino acids contributed by both subunits of the dimer, only the aminoglycoside affects the

dx.doi.org/10.1021/bi301126g | *Biochemistry* 2012, 51, 9147−9155

monomer−dimer equilibrium of the enzyme by favoring dimer formation. A large excess of aminoglycosides does not cause any further aggregation, indicating that the dimer formation is specific and relevant to the catalytic activity of the enzyme. This is also consistent with kinetic data that showed that the aminoglycoside substrate binds first to the enzyme. Surprisingly, divalent cations also shifted the equilibrium toward the dimer formation through the aminoglycoside binding site, in contrast to no effect by Mg-ATP. Such a ligand-dependent monomer−dimer equilibrium has not been observed with any other AGME.

Binding of aminoglycosides to ANT occurs with a favorable enthalpy and unfavorable entropy, yielding an overall favorable Gibbs energy. This is similar to the observations with other AGMEs. The size of aminoglycosides has a significant effect on the binding enthalpy, and the presence of the fourth ring on aminoglycosides renders the binding significantly more favorable. These studies also showed that ANT is the least capable AGME characterized to date to discriminate the substitution at the C2′ site of the aminoglycosides (kanamycin A vs kanamycin B). The most significant effects are observed with the changes in the substitution at the C6′ site (neomycin vs paromomycin), which is the most distant position from the nucleotidylation site.

■ ASSOCIATED CONTENT

Supporting Information

Two figures showing free- and enzyme-bound EPR spectra for Mn^{2+} and data acquired by analytical ultracentrifugation showing the effect of salt concentration on the monomer−dimer equilibrium of the enzyme. This material is available free of charge via the Internet at http://pubs.acs.org.

■ AUTHOR INFORMATION

Corresponding Author

*Department of Biochemistry and Cellular and Molecular Biology, The University of Tennessee, Walters Life Sciences Building, M 407, Knoxville, TN 37996-0840. Telephone: (865) 974-2668. Fax: (865) 974-6306. E-mail: serpersu@utk.edu.

Funding

This work is supported by a grant from the National Science Foundation (MCB-0842743 to E.H.S.). B.D.B. was partially supported by National Science Foundation Grant DBI-0403781.

Notes

The authors declare no competing financial interest.

■ ACKNOWLEDGMENTS

B.D.B. thanks Dr. M. Ishiura and Dr. K. Onai from the Center for Gene Research at Nagoya University (Nagoya, Japan) for the generous gift of pCkm_{Te}.

■ ABBREVIATIONS

AG, aminoglycoside; AGME, aminoglycoside-modifying enzyme; ANT, aminoglycoside nucleotidyltransferase (4′); EPR, electron paramagnetic resonance; ITC, isothermal titration calorimetry; AUC, analytical ultracentrifugation; IPTG, isopropyl β-D-1-thiogalactopyranoside; MOPS, 3-(*N*-morpholino)propanesulfonic acid; MES, 2-(*N*-morpholino)-ethanesulfonic acid; HEPES, 4-(2-hydroxyethyl)-1-piperazineethanesulfonic acid; PIPES, 1,4-piperazinediethanesulfonic acid; BICINE, glycine, *N*,*N*-bis(2-hydroxyethyl)-; Tris, 1,3-propanediol, 2-amino-2-(hydroxymethyl)-.

■ REFERENCES

(1) Spotts, C. R., and Stanier, R. Y. (1961) Mechanism of Streptomycin Action on Bacteria: Unitary Hypothesis. *Nature 192*, 633−637.

(2) Davies, J. E. (1991) Aminoglycoside-Aminocyclitol Antibiotics and Their Modifying Enzymes. In *Antibiotics in Laboratory Medicine* (Lorian, V., Ed.) 4th ed., p 1283, Lippincott Williams & Wilkins, Philadelphia.

(3) Shaw, K. J., Rather, P. N., Hare, R. S., and Miller, G. H. (1993) Molecular-Genetics of Aminoglycoside Resistance Genes and Familial Relationships of the Aminoglycoside-Modifying Enzymes. *Microbiol. Rev. 57*, 138−163.

(4) Wright, G. D. (1999) Aminoglycoside-modifying enzymes. *Curr. Opin. Microbiol. 2*, 499−503.

(5) Gates, C. A., and Northrop, D. B. (1988) Substrate Specificities and Structure Activity Relationships for the Nucleotidylation of Antibiotics Catalyzed by Aminoglycoside Nucleotidyltransferase-2″-I. *Biochemistry 27*, 3820−3825.

(6) Chen-Goodspeed, M., Vanhooke, J. L., Holden, H. M., and Raushel, F. M. (1999) Kinetic mechanism of kanamycin nucleotidyltransferase from *Staphylococcus aureus*. *Bioorg. Chem. 27*, 395−408.

(7) Revuelta, J., Corzana, F., Bastida, A., and Asensio, J. (2010) The Unusual Nucleotide Recognition Properties of the Resistance Enzyme ANT(4′): Inorganic Tri/Polyphosphate as a Substrate for Aminoglycoside Inactivation. *Chem.—Eur. J. 16*, 8635−8640.

(8) Revuelta, J., Vacas, T., Torrado, M., Corzana, F., Gonzalez, C., Jimenez-Barbero, J., Menendez, M., Bastida, A., and Asensio, J. L. (2008) NMR-based analysis of aminoglycoside recognition by the resistance enzyme ANT(4′): The pattern of OH/NH_3^+ substitution determines the preferred antibiotic binding mode and is critical for drug inactivation. *J. Am. Chem. Soc. 130*, 5086−5103.

(9) Wright, E., and Serpersu, E. H. (2006) Molecular determinants of affinity for aminoglycoside binding to the aminoglycoside nucleotidyltransferase(2″)-Ia. *Biochemistry 45*, 10243−10250.

(10) Wright, E., and Serpersu, E. H. (2005) Enzyme-substrate interactions with an antibiotic resistance enzyme: Aminoglycoside nucleotidyltransferase(2″)-Ia characterized by kinetic and thermodynamic methods. *Biochemistry 44*, 11581−11591.

(11) Matsumura, M., Katakura, Y., Imanaka, T., and Aiba, S. (1984) Enzymatic and nucleotide sequence studies of a kanamycin-inactivating enzyme encoded by a plasmid from thermophilic bacilli in comparison with that encoded by plasmid pUB110. *J. Bacteriol. 160*, 413−420.

(12) Onai, K., Morishita, M., Kaneko, T., Tabata, S., and Ishiura, M. (2004) Natural transformation of the thermophilic cyanobacterium *Thermosynechococcus elongatus* BP-1: A simple and efficient method for gene transfer. *Mol. Gen. Genet. 271*, 50−59.

(13) Sakon, J., Liao, H. H., Kanikula, A. M., Benning, M. M., Rayment, I., and Holden, H. M. (1993) Molecular-Structure of Kanamycin Nucleotidyltransferase Determined to 3.0-Å Resolution. *Biochemistry 32*, 11977−11984.

(14) Pedersen, L. C., Benning, M. M., and Holden, H. M. (1995) Structural investigation of the antibiotic and ATP-binding sites in kanamycin nucleotidyltransferase. *Biochemistry 34*, 13305−13311.

(15) Lundblad, R. L., Kingdon, H. S., and Mann, K. G. (1976) Thrombin. *Methods Enzymol. 45*, 156−176.

(16) Schuck, P. (2000) Size-distribution analysis of macromolecules by sedimentation velocity ultracentrifugation and Lamm equation modeling. *Biophys. J. 78*, 1606−1619.

(17) Laue, T. M., Shah, B. D., Ridgeway, T. M., and Pelletier, S. L. (1992) in *Analytical Ultracentrifugation in Biochemistry and Polymer Science* (Harding, S. E., Rowe, A. J., and Horton, J. C., Eds.) pp 90−125, Royal Society of Chemistry, Cambridge, U.K.

(18) Schuck, P. (2003) On the analysis of protein self-association by sedimentation velocity analytical ultracentrifugation. *Anal. Biochem. 320*, 104−124.

(19) Brautigam, C. A. (2011) Using Lamm-equation modeling of sedimentation velocity data to determine the kinetic and thermodynamic properties of macromolecular interactions. *Methods 54*, 4−15.
(20) Dam, J., Velikovsky, C. A., Mariuzza, R. A., Urbanke, C., and Schuck, P. (2005) Sedimentation velocity analysis of heterogeneous protein-protein interactions: Lamm equation modeling and sedimentation coefficient distributions c(s). *Biophys. J. 89*, 619−634.
(21) Norris, A. L., Ozen, C., and Serpersu, E. H. (2010) Thermodynamics and Kinetics of Association of Antibiotics with the Aminoglycoside Acetyltransferase (3)-IIIb, a Resistance-Causing Enzyme. *Biochemistry 49*, 4027−4035.
(22) Wiseman, T., Williston, S., Brandts, J. F., and Lin, L. N. (1989) Rapid Measurement of Binding Constants and Heats of Binding Using a New Titration Calorimeter. *Anal. Biochem. 179*, 131−137.
(23) Ozen, C., Malek, J. M., and Serpersu, E. H. (2006) Dissection of aminoglycoside-enzyme interactions: A calorimetric and NMR study of neomycin B binding to the aminoglycoside phosphotransferase(3′)-IIIa. *J. Am. Chem. Soc. 128*, 15248−15254.
(24) Norris, A. L., and Serpersu, E. H. (2010) Interactions of Coenzyme A with the Aminoglycoside Acetyltransferase (3)-IIIb and Thermodynamics of a Ternary System. *Biochemistry 49*, 4036−4042.
(25) Özen, C., and Serpersu, E. H. (2004) Thermodynamics of aminoglycoside binding to aminoglycoside-3′-phosphotransferase IIIa studied by isothermal titration calorimetry. *Biochemistry 43*, 14667−14675.
(26) Wright, E., and Serpersu, E. H. (2006) Molecular determinants of affinity for aminoglycoside binding to the aminoglycoside nucleotidyltransferase (2″)-Ia. *Biochemistry 45*, 10243−10250.
(27) Boehr, D. D., Farley, A. R., LaRonde, F. J., Murdock, T. R., Wright, G. D., and Cox, J. R. (2005) Establishing the principles of recognition in the adenine-binding region of an aminoglycoside antibiotic kinase APH(3′)-IIIa. *Biochemistry 44*, 12445−12453.
(28) Hedge, S. S., Dam, T. K., Brewer, C. F., and Blachard, J. S. (2002) Thermodynamics of aminoglycoside and acyl-coenzyme A binding to the salmonella enterica AAC(6′)-Iy aminoglycoside N-acetyltransferase. *Biochemistry 41*, 7519−7527.
(29) Serpersu, E. H., and Norris, A. L. (2012) Effect of Protein Dynamics and Solvent in Ligand Recognition by Promiscuous Aminoglycoside-Modifying Enzymes. In *Advances in Carbohydrate Chemistry and Biochemistry* (Derek, H., Ed.) pp 221−248, Academic Press, New York.
(30) Pimentel, G. C., and Mcclella, A. (1971) Hydrogen Bonding. *Annu. Rev. Phys. Chem. 22*, 347.
(31) Habermann, S. M., and Murphy, K. P. (1996) Energetics of hydrogen bonding in proteins: A model compound study. *Protein Sci. 5*, 1229−1239.